Effects of Thiophene Units on Substituted Benzothiadiazole and Benzodithiophene Copolymers for Photovoltaic Applications

Ping Ding,[1] Yingping Zou,[1] Cheng-Che Chu,[2] Dequan Xiao,[3] Chain-Shu Hsu[2]

[1]*College of Chemistry and Chemical Engineering, Central South University, Changsha 410083, China*
[2]*Department of Applied Chemistry, National Chiao Tung University, Hsinchu 30010, Taiwan*
[3]*Department of Chemistry, Yale University, 225 Prospect Street, New Haven, Connecticut 06520-8107*

Received 5 August 2011; accepted 21 November 2011
DOI 10.1002/app.36541
Published online 29 February 2012 in Wiley Online Library (wileyonlinelibrary.com).

ABSTRACT: Two conjugated copolymers, poly{4,7-[5,6-bis(octyloxy)]benzo(c)(1,2,5)thiadiazole-*alt*-4,8-di(2-ethylhexyloxyl)benzo[1,2-*b*:3,4-*b*]dithiophene} (**P1**) and poly(2-{5-[5,6-bis(octyloxy)-4-(thiophen-2-yl)benzo(c)(1,2,5)thiadiazol-7-yl] thiophen-2-yl}-4,8-di(2-ethylhexyloxyl)benzo(1,2-*b*:3,4-*b*)dithiophene) (**P2**), composed of benzodithiophene and 5,6-dioctyloxybenzothiadiazole derivatives with or without thiophene units were synthesized via a Stille cross-coupling polymerization reaction. These copolymers are promising for applications in bulk heterojunction solar cells because of their good solubility, proper thermal stability, moderate hole mobility, and low band gap. The photovoltaic properties of these copolymers were investigated on the basis of blends of the different polymer/(6,6)-phenyl-C_{71}-butyric acid methyl ester ($PC_{71}BM$) weight ratios under AM1.5G illumination at 100 mW/cm^2. The device with indium tin oxide/poly(3,4-ethylene dioxythiophene):poly(styrene sulfonate)/**P2**:$PC_{71}BM$ (1 : 2 w/w)/Ca/Al gave a relatively better photovoltaic performance with a power conversion efficiency of 1.55%. © 2012 Wiley Periodicals, Inc. J Appl Polym Sci 125: 3936–3945, 2012

Key words: copolymerization; NLO; synthesis

INTRODUCTION

In the past 2 decades, polymer solar cells (PSCs) have attracted broad interests because of their flexibility and low cost of processing.[1–3] Conjugated polymers with low band gaps are emerging as competitive candidates for the development of PSCs into practical applications because of the improved absorption of solar photon flux for generating a higher photocurrent.[4] In recent years, bulk heterojunction PSCs have made great progress.[5–7] In these types of device, a blend of an electron-donating material (*p*-type conjugated polymers) and an electron-accepting material (*n*-type fullerene derivatives) is used as the active layer. One representative bulk heterojunction PSC is a device based on a blend of benzodithiophene (BDT)-based conjugated polymers as electron donors and a soluble C_{70} derivative, (6,6)-phenyl-C_{71}-butyric acid methyl ester ($PC_{71}BM$), as an electron acceptor.[8,9] In 2009, Hou et al.[10] reported a power conversion efficiency (PCE) of PSCs based on FPBDTTT–CF that reached up to 7.7%. In 2010, Leclerc et al.[11] synthesized a new BDT-based polymer (PBDTTPD) using thienopyrrodione as the new electron-accepting unit, with a low band gap and preferred energy level; it exhibited a high PCE up to 5.5% with a large active area of 1 cm^2. Therefore, alternating donor–acceptor (D–A) poly(2,6-benzodithiophene) derivatives with a suite of electron-accepting moieties is particularly interesting for the development of PSCs.

As electron-donor materials, conjugated polymers are usually required to carry flexible side chains to ensure polymers with good solubility in organic solvents. The lengths and positions of alkyl or alkoxyl chains play an important role in the solubility, molecular weight, and energy level of conjugated polymers, the morphologies of blend films, and, therefore, the photovoltaic performance of devices.[12,13] Our group recently synthesized a copolymer, namely, poly(2-{5-[5,6-bis(octyloxy)-4-(thiophen-2-yl)benzo(c)(1,2,5)thiadiazol-7-yl]thiophen-2-yl}-4,8-di(2-ethylhexyloxyl)-benzo(1,2-*b*:3,4-*b*)dithiophene) (PBDT–DODTBT or **P2**), with two octyloxy chains on a benzothiadiazole moiety; this polymer demonstrated that a

Correspondence to: Y. Zou (yingpingzou@csu.edu.cn).
Contract grant sponsor: Lieying Project, the Fundamental Research Funds for the Central Universities; contract grant number: 2010QZZD0112.
Contract grant sponsor: Doctoral Fund of Ministry of Education of China; contract grant number: 20100162120033.
Contract grant sponsor: Opening Fund of State Key Laboratory of Powder Metallurgy.
Contract grant sponsor: NSFC (Nos. 51173206, 21161160443, 51150110158).

© 2012 Wiley Periodicals, Inc.

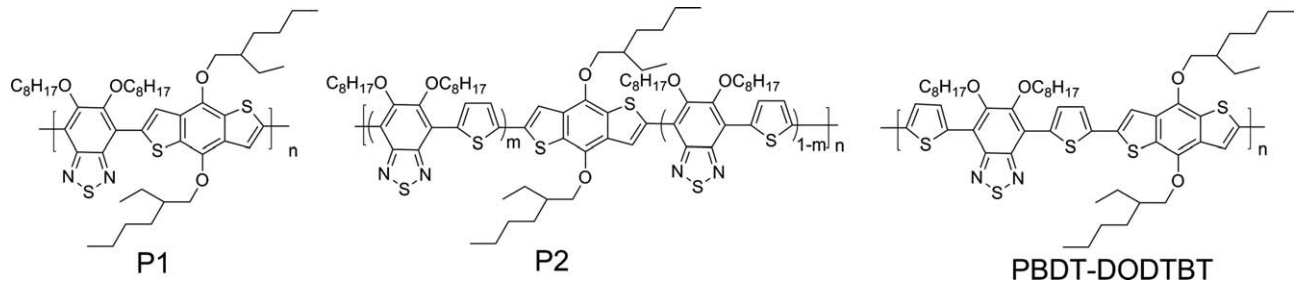

Scheme 1 The structures of the corresponding polymers.

planar structure was formed because of the low steric hindrance of the octyloxy chain, and a PCE of 4% was achieved.[14] The results indicated that 5,6-dioctyloxybenzothiadiazole (DOBT) was a good electron-accepting building block to construct highly soluble polymer photovoltaic materials.

As is well known, polythiophene and its derivatives have been investigated as active materials for wide applications in polymer light-emitting diodes, polymer field-effect transistors, and PSCs because of their relatively higher hole mobility in comparison with other conjugated polymers.[15–17] Obviously, the thiophene unit was very important in tuning the optoelectronic properties of the polymers. Moreover, to the best of our knowledge, there has been no report on the incorporation of one thiophene unit into DOBT moiety to construct polymers for photovoltaic applications or to investigate the effect of changes in the numbers of thiophene units on the thermal, optical, electrochemical, and photovoltaic properties of DOBT-based polymers. On the basis of the these considerations and our previous work, we synthesized two conjugated polymers, poly{4,7-[5,6-bis(octyloxy)]benzo(c)(1,2,5)thiadiazole-*alt*-4,8-di(2-ethylhexyloxyl)benzo[1,2-*b*:3,4-*b*]dithiophene} (**P1**) without thiophene unit and **P2** with one thiophene unit in the repeating unit, as shown in Scheme 1; both polymers used DOBT as an electron-deficient moiety and BDT as an electron-rich moiety. A similar polymer, PBDT–DODTBT, is also listed for comparison.[14] In this work, from **P1** to PBDT–DODTBT, the hole mobilities and PCEs of the polymer/$PC_{71}BM$ blends gradually increased with increasing addition of thiophene units. Furthermore, the relationship between the structure and the optoelectronic properties was also investigated and is discussed in detail.

EXPERIMENTAL

Materials

Tetrakis(triphenylphosphine)palladium ($Pd(PPh_3)_4$), 2-thiophene boronic acid, and catechol were obtained from Alfa Asia Chemical Co. and Pacific Chem Source, Zhengzhou, China, and they were used as received. Toluene was dried over Na/benzophenone ketyl and was freshly distilled before use. Other reagents and solvents were purchased commercially as analytical-grade quality and were used without further purification. Column chromatography was carried out on silica gel (size = 200–300 mesh). 2,6-Bis(trimethyltin)-4,8-di(2-ethylhexyloxyl)-benzo(1,2-*b*:3,4-*b*)dithiophene (**4**) was prepared according to the literature.[18,19]

Characterization

^{1}H-NMR spectra were recorded with a Bruker AV-400 spectrometer in deuterated chloroform solution at 298 K, unless otherwise specified. The chemical shifts are reported as δ values (parts per million) relative to an internal tetramethylsilane standard. Elemental analysis was performed on a Flash EA 1112 analyzer. The molecular weight and polydispersity index (PDI) values of the polymer were determined by gel permeation chromatography analysis with polystyrene as the standard [a Waters 515 high-performance liquid chromatography (HPLC) pump, a Waters 2414 differential refractometer, and three Waters Styragel columns (HT2, HT3, and HT4)] with tetrahydrofuran (HPLC grade) as the eluent at a flow rate of 1.0 mL/min at 35°C. Thermogravimetric analysis (TGA) was conducted on a Shimadzu DTG-60 thermogravimetric analyzer at a heating rate of 20°C/min under a nitrogen atmosphere. The temperature of degradation corresponded to a 5% weight loss. The ultraviolet–visible absorption spectra were recorded on a Jasco V-570 spectrophotometer. For solid-state measurements, the polymer solution in chloroform was drop-cast onto quartz plates. The optical band gap was calculated from the onset of the absorption spectra. X-ray diffraction (XRD) measurements of the polymer thin films were carried out with a 2-kW Rigaku XRD system. XRD patterns were obtained with Bragg–Brentano geometry (θ–2θ) with Cu Kα radiation as an X-ray source in the reflection mode at 45 kV and 300 mA. The cyclic voltammogram was recorded with a Zahner IM6e electrochemical workstation (Germany) with polymer film on a platinum disk as the working

electrode, platinum wire as the counter electrode, and Ag/Ag^+ (0.1*M*) as the reference electrode in a nitrogen-saturated acetonitrile (CH_3CN) solution containing 0.1 mol/L tetrabutylammonium hexafluorophosphate (Bu_4NPF_6). The hole mobility of the polymer was measured by the space-charge-limited current (SCLC) method with a device structure of indium tin oxide (ITO)/poly(3,4-ethylene dioxythiophene) (PEDOT):poly(styrene sulfonate) (PSS)/polymer/Au. The morphology of the polymer/PCBM ([6,6]-phenyl-C61-butyric acid methyl ester) blend films was investigated by a SPI 3800N atomic force microscopy (AFM) instrument (Seiko Instruments Inc. Japan) in contacting mode with a 1-μm scanner.

Fabrication and characterization of the photovoltaic cells

The PSCs were fabricated in the configuration of the common sandwich structure with an ITO glass anode and a calcium/aluminum cathode. Patterned ITO glass with a sheet resistance of 15–20 Ω/□ was purchased from CSG Holding Co., Ltd. (China). Each ITO substrate was patterned with photolithography techniques. Before use, the substrates were cleaned with detergent and deionized water. Then, they were ultrasonicated in acetone and isopropyl alcohol for 15 min, respectively. The ITO substrates were subjected to UV ozone cleaning for 15 min. The ITO substrates were spin-coated (3500 rpm, 60 s) with a thin film (25 nm) of (PEDOT:PSS, Al4083, H. C. Stark) and dried at 150°C for 30 min in a glovebox. A blend of C_{71}–PCBM (Nano-C) and the polymer was solubilized in *o*-dichlorobenzene overnight, filtered through a 0.45-μm polytetrafluoroethylene filter, and then spin-coated at 2000 rpm for 60 s onto the PEDOT:PSS layer. Sequentially, the devices were completed by deposition of a 10-nm Ca and 100-nm Al layer. This layer was thermally evaporated at a pressure of 6×10^{-1} Torr at room temperature. Solar cells were fabricated with an effective area of 0.12 cm^2. The current versus potential curves (*I–V* characteristics) were measured with a Keithley 2400 digital source meter under an acollimated beam. The illumination of the cells was done through the ITO side with light from a 300-W San-Ei solar simulator (XES-301S + EL-100) to provide an intensity of 100 mW/cm^2. All fabrications after the cleaning of the ITO substrates and characterizations were performed in a glovebox.

Synthesis of the monomers and polymers

The synthetic routes of the monomers and polymers are shown in Scheme 2. The dibromonated monomer, 4,7-dibromo-5,6-bis(octyloxy)benzo(c)(1,2,5)thiadiazole (**1**), was synthesized according to our recent publication.[14] All of the other compounds were synthesized by the following procedures.

4-Bromo-5,6-bis(octyloxy)-7-(thiophen-2-yl) benzo(c)(1,2,5)thiadiazole (**2**)

Compound **1** (4.13 g, 7.5 mmol), 2-thiophene boronic acid (2.50 g, 19.5 mmol), 1*M* $NaHCO_3$ (75 mL), and $CH_3OCH_2CH_2OCH_3$ (75 mL) were carefully degassed, and then, $Pd(PPh_3)_4$ (0.1156 g, 0.1 mmol) was added. The reaction mixture was stirred at 90°C under a nitrogen atmosphere for 12 h. After the completion of the reaction, the reaction mixture was poured into ice water, and the water phase was extracted with dichloromethane three times. The combined organic phase was washed with NaOH (aqueous), and the solvents were evaporated under reduced pressure. The crude product was purified on a silica gel column eluted with CH_2Cl_2/hexane (1 : 10 v/v). A yellow green oil was obtained.

Yield: 2.65 g (64%). ^{1}H-NMR (400 MHz, $CDCl_3$, ppm, δ): 8.48–8.47 (d, 1H), 7.52–7.51 (d, 1H), 7.24–7.23 (t, 1H), 4.09–4.12 (t, 4H), 1.88–1.96 (m, 4H), 1.41–1.29 (m, 20H), 0.91–0.88 (t, 6H). ANAL. Calcd for $C_{26}H_{37}BrN_2O_2S_2$: C, 56.41%; H, 6.74%; N, 5.06%. Found: C, 56.42%; H, 6.76%; N, 5.02%.

4-Bromo-5,6-bis(octyloxy)-7-(5-bromothiophen-2-yl)benzo(c)(1,2,5)thiadiazole (**3**)

A mixture of **2** (2.76 g, 5 mmol), *N*-bromosuccimide (1.96 g, 11 mmol), glacial acetic acid (100 mL), and chloroform (100 mL) was stirred at room temperature in the dark for 24 h. The solvent was removed under reduced pressure, and the residue was chromatographically purified on a silica gel column eluted with CH_2Cl_2/hexane (1 : 10 v/v) to afford **3** as a yellow crystal (2.56 g, 81%).

^{1}H-NMR (400 MHz, $CDCl_3$, ppm, δ): 8.35–8.34 (d, 1H), 7.17–7.16 (d, 1H), 4.17–4.12 (t, 4H), 1.93–1.91 (m, 4H), 1.37–1.30 (m, 20 H), 0.91–0.88 (t, 6H). ANAL. Calcd for $C_{26}H_{36}Br_2N_2O_2S_2$: C, 49.37%; H, 5.34%; N, 4.43%. Found: C, 49.40%; H, 5.37%; N, 4.48%.

P1

1 (110.0 mg, 0.2 mmol) and **4** (154.4 mg, 0.2 mmol) were dissolved in toluene (6 mL). The solution was flushed with argon for 10 min, and then, $Pd(PPh_3)_4$ (20 mg, 0.016 mmol) was added to the flask. The flask was purged three times with successive vacuum and argon filling cycles. The polymerization reaction was heated to 100°C, and the mixture was stirred for 48 h under an argon atmosphere. The mixture was cooled to room temperature and poured slowly in methanol (100 mL); the resulting precipitate was collected by filtration. The crude polymer was washed with methanol and hexane in

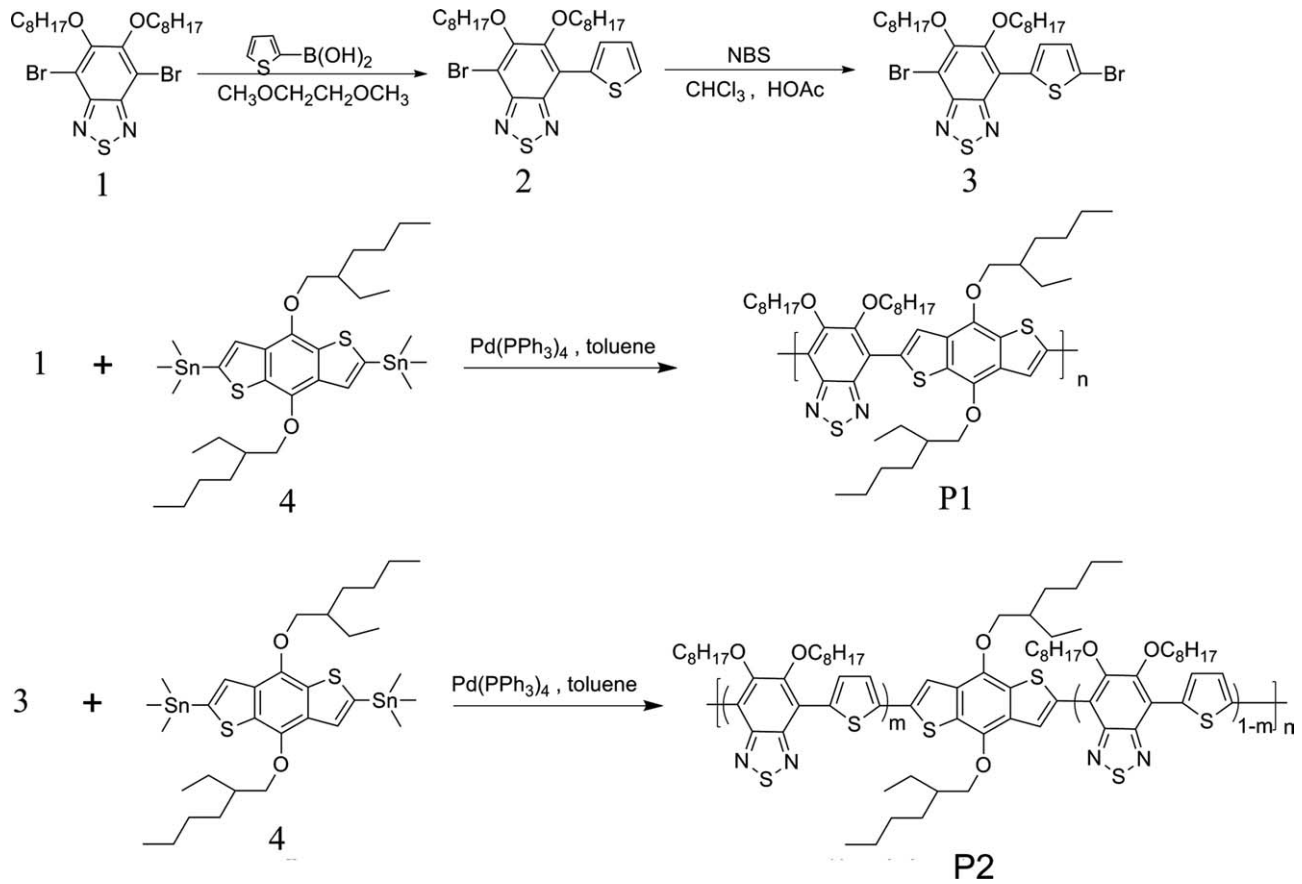

Scheme 2 Structures and synthetic routes of the polymers.

a Soxhlet apparatus to remove the oligomers and catalyst residue. Finally, the polymer was extracted with chloroform. The polymer solution was condensed to about 20 mL and slowly poured into methanol (200 mL). The precipitate was collected by filtration and dried under a high vacuum to afford **P1** as a purple solid (0.145 g, 84%).

^{1}H-NMR (400 MHz, $CDCl_3$, ppm, δ): 8.32–8.25 (br, 2H), 4.21–3.96 (br, 8H), 2.23–1.05 (br, 42H), 0.92–0.89 (br, 18H). ANAL. Calcd for $(C_{48}H_{70}S_3N_2O_4)_n$: C, 69.02%; H, 8.45%; N, 3.35%. Found: C, 69.04%; H, 8.42%; N, 3.35%. Number-average molecular weight (M_n) = 23,115; weight-average molecular weight (M_w) = 39,015; PDI = 1.69.

P2

P2 was synthesized with a procedure similar to that used for **P1** from monomer **3** (126.4 mg, 0.2 mmol) and monomer **4** (154.4 mg 0.2 mmol); it was a dark purple solid of 154 mg.

Yield: 78%.^{1}H-NMR (400 MHz, $CDCl_3$, ppm, δ): 8.36–8.17 (br, 3H), 7.25–7.21 (br, 1H), 4.20–3.97 (br, 8H), 2.21–1.06 (br, 42H), 0.92–0.90 (br, 18H). ANAL. Calcd for $(C_{52}H_{72}S_4N_2O_4)_n$: C, 68.08%; H, 7.91%; N, 3.05%. Found: C, 68.09%; H, 7.93%; N, 3.08%. M_n = 6473; M_w = 15,098; PDI = 2.33.

RESULTS AND DISCUSSION

Synthesis and characterization

Two BDT–benzothiadiazole copolymers with different numbers of thiophene units were synthesized via the Stille polymerization reaction. The structures and synthetic routes of the polymers are outlined in Scheme 2. The polymers were purified by a sequential Soxhlet extraction with methanol, hexanes, and $CHCl_3$. The $CHCl_3$ fraction was then reduced in volume, precipitated into methanol, and collected by filtration to yield a purple (**P1**) or dark purple (**P2**) solid. It worth noting that **P1** was an alternating polymer and **P2** was a random polymer, in that this polymerization resulted in both head–head and head–tail connections with regard to the asymmetric monomer unit in the main chain. The structure and preliminary photovoltaic properties of PBDT–DODTBT were published previously in the literature.[14] The chemical structures of the comonomers and the polymers were verified by ^{1}H-NMR and elemental analysis. The molecular weight of the

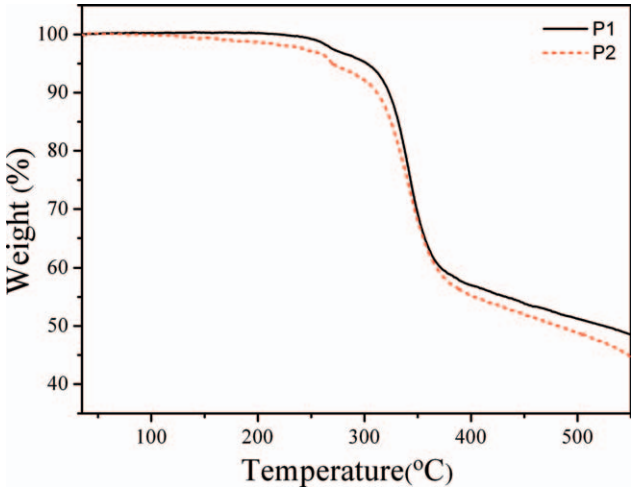

Figure 1 TGA curves of **P1** and **P2** at a scan rate of 20°C/min under a nitrogen atmosphere. [Color figure can be viewed in the online issue, which is available at wileyonlinelibrary.com.]

polymer was determined by gel permeation chromatography in a tetrahydrofuran solution relative to polystyrene standards. The M_n values of **P1** and **P2** were 23.1 and 6.5 kg/mol with PDI values of 1.69 and 2.33, respectively. The relatively low M_n's for polymer **P2** and PBDT–DODTBT were probably due to the relatively poor solubility in the organic solvents used in the polycondensation reaction. They were precipitated from the reaction mixture during the polycondensation process. The precipitated polymers were readily soluble in common solvents such as chloroform and 1,2-dichlorobenzene. The thermal stability of the polymers were investigated with TGA, as shown in Figure 1. TGA revealed that the 5% weight loss temperatures (degradation temperature) of **P1** and **P2** were 302 and 271°C, respectively. This indicated that the thermal stability of the copolymers would be good for optoelectronic applications.

Optical properties

The normalized absorption spectra of polymers **P1, P2** and PBDT–DODTBT in $CHCl_3$ solutions and the films are shown in Figure 2(a,b), respectively. The related optical data are summarized in Table I. The polymers generally showed two absorption peaks, both in chloroform solution and in the thin film; this was in accordance with the other D–A copolymers.[20] The absorption maxima of **P1** in the chloroform solution was about 570 nm; this was redshifted in comparison with those of the other two polymers (the absorption peaks of the **P2** and PBDT–DODTBT solutions were located at 553 and 548 nm, respectively). This was mainly caused by the fact that the electron-rich thiophene unit weakened the intramolecular charge transfer (ICT) on the conjugated polymer backbone. As shown in Figure 2, the absorption spectra of polymers **P1, P2,** and PBDT–DODTBT in the thin films were broadened and redshifted in comparison with those of the solution. The broader and better absorption originated from the stronger electronic interaction between the individual polymer chains in the film states. The absorption onset wavelengths of **P1, P2,** and PBDT–DODTBT were 732, 746, and 758 nm; these values corresponded to optical band gaps of 1.69, 1.66, and 1.64 eV, respectively. The optical band gaps of the polymers are summarized in Table I. The results show that the number of thiophene units did not affect the optical band gap of these kind of polymers.

Electrochemical properties

Cyclic voltammetry is usually applied to estimate the highest occupied molecular orbital (HOMO) and lowest unoccupied molecular orbital (LUMO) levels

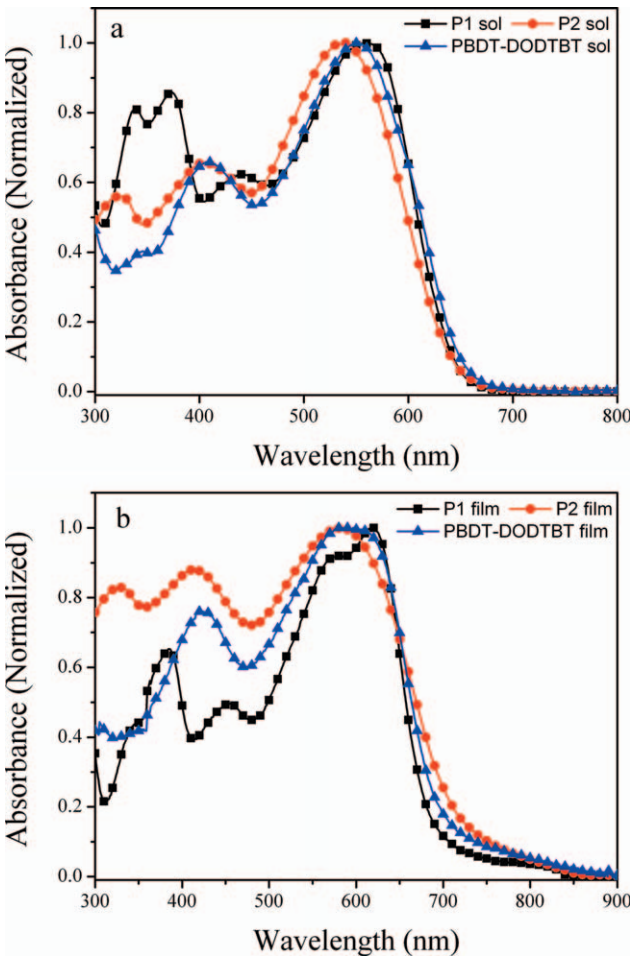

Figure 2 Normalized absorption spectra of **P1, P2,** and PBDT–DODTBT in the (a) $CHCl_3$ and (b) thin films. [Color figure can be viewed in the online issue, which is available at wileyonlinelibrary.com.]

TABLE I
Optical and Electrochemical Properties of the Polymers

	Absorption spectra				Cyclic voltammetry (vs Ag/Ag^+)		
	Solution[a]	Film[b]			*p* Doping	*n* Doping	
Polymer	λ_{max} (nm)	λ_{max} (nm)	λ_{onset} (nm)	E_g^{op} (eV)[c]	E_{on}^{ox} (V)/HOMO (eV)	E_{on}^{red} (V)/LUMO (eV)	E_g^{EC} (eV)
P1	570	620	732	1.69	0.46/−5.17	−1.22/−3.49	1.68
P2	553	571	746	1.66	0.47/−5.18	−1.14/−3.57	1.61
PBDT–DODTBT	548	600	758	1.64	0.46/−5.17	−1.10/−3.61	1.56

[a] Measured in a chloroform solution.
[b] Cast from a chloroform solution.
[c] Band gap estimated from the onset wavelength of the optical absorption.[22]

of conjugated polymers. The onset oxidation potential (E_{ox}) and onset reduction potential (E_{red}) obtained from cyclic voltammograms correspond to the HOMO and LUMO energy levels, respectively. The electrochemical properties of the two copolymers were investigated by cyclic voltammetry, as shown in Figure 3. All of the potentials are reported with Ag/Ag^+ as the reference with the ferrocene/ferrocenium couple as an internal standard, and the correlation can be expressed as follows:[21]

$$\text{HOMO} = -e(E_{on}^{ox} + 4.71)(\text{eV})$$

$$\text{LUMO} = -e(E_{on}^{red} + 4.71)(\text{eV})$$

Where E_{ox} is the onset oxidation potential and E_{red} is the onset reduction potential. As observed from the cyclic voltammograms in Figure 3, the two copolymers exhibited partially reversible oxidation and irreversible reduction processes. The E_{ox} values were observed to be 0.46 and 0.47 V for **P1** and **P2,** respectively. In addition, the E_{red} values were found to be −1.22 and −1.14 V, respectively. From the values of E_{ox} and E_{red}, the HOMO and LUMO energy levels and electrochemical band gaps (E_g's) of the copolymers were calculated, and the results are shown in Table I. The corresponding E_g values were similar to the optical band gaps within the experimental error. We found that the E_{ox} values of **P1, P2,** and PBDT–DODTBT were similar; this indicated that the HOMO levels of the three polymers were mainly determined by the BDT segments. Compared with **P1, P2,** by the incorporation of one thiophene unit, and PBDT–DODTBT, by the incorporation of two thiophene units, were found to possess higher E_{red} values.

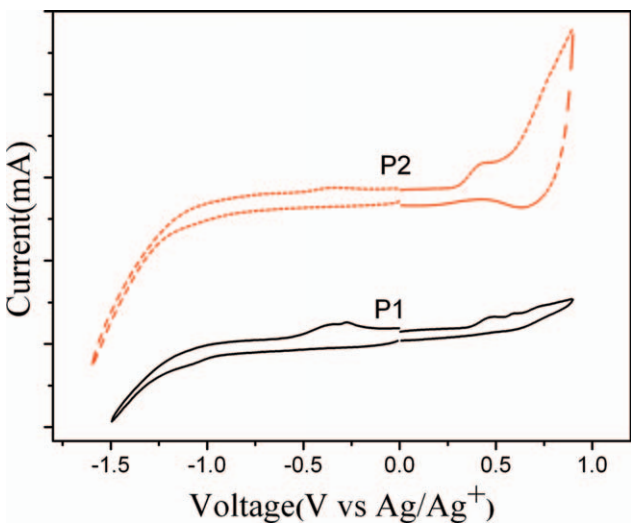

Figure 3 Cyclic voltammograms of the copolymer films on a platinum electrode in 0.1 mol/L Bu_4NPF_6 and CH_3CN solution. [Color figure can be viewed in the online issue, which is available at wileyonlinelibrary.com.]

Theoretical calculations

The optimal geometries and electronic state wave function distributions of HOMO and LUMO of the D–A model compound were obtained at the density functional theory (DFT B3LYP/6-31G*) level with a Gaussian 03 program suite[23] (Fig. 4). To simplify the calculations, all of the alkyl chains were replaced by —CH_3 groups. DFT B3LYP/6-31G* has been found to be an accurate method for calculating the optimal geometry and electronic structures of many molecular systems without consideration of the solvent effect and interactions between polymer chains. *Ab initio* calculations for model compound **1** for **P1** and model compound **2** for **P2** showed that the two copolymers were planar; this enabled the electrons to be delocalized within the entire molecule because of π conjugation. For **P1** and **P2,** the electronic wave function of HOMO was distributed entirely over the conjugated molecules; this was beneficial for obtaining a higher hole mobility;[24] however, the electron wave function of LUMO was mainly localized on the DOBT part. Thus, the incorporation of the DOBT segment effectively reduced the band gap because of the low LUMO energy level of the DOBT unit. From the DFT B3LYP/6-31G* level calculations combined with the equations provided by Leclerc's group,[25] the HOMO and LUMO energy levels of **P1** were

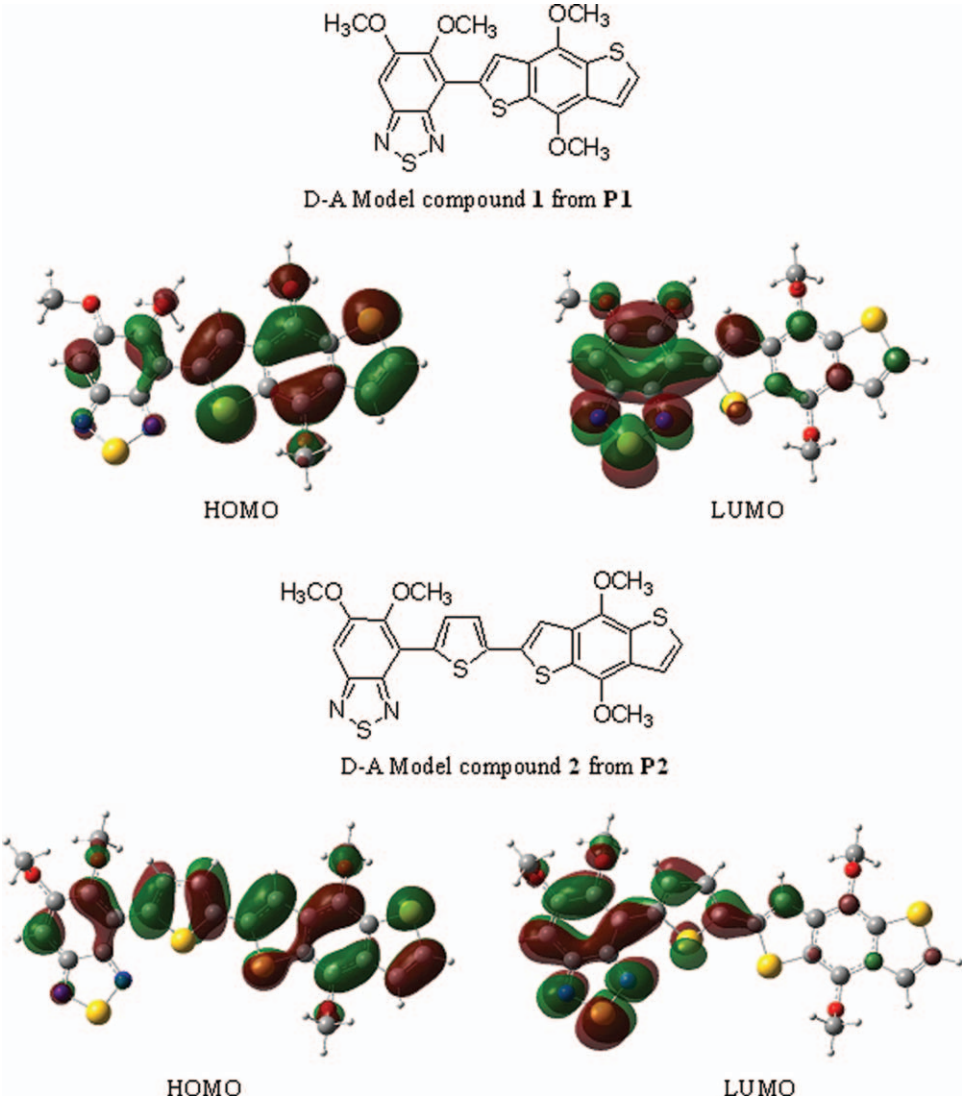

Figure 4 Molecular orbital isosurfaces of HOMO and LUMO of the model compounds from **P1** and **P2** calculated at the DFT B3LYP/6-31G* level. [Color figure can be viewed in the online issue, which is available at wileyonlinelibrary.com.]

−5.21 and −3.45 eV, and the HOMO and LUMO energy levels of **P2** were −5.22 and −3.53 eV, respectively. These values were in good agreement with the experimental values for the energy gap and the HOMO and LUMO energy levels. Therefore, the DFT calculations performed on the repetitive units provided good estimations of the HOMO, LUMO, and band-gap energy trends and allowed rapid screening of the promising polymeric structures.

Hole mobility

Hole mobility is another important parameter of conjugated polymers for photovoltaic applications. We measured the hole mobilities of **P1** and **P2** with the SCLC model using a device structure of ITO/PEDOT:PSS/active layer (170 nm)/Au (100 nm). The results are plotted as $\ln(Jd^3/V^2)$ versus $(V/d)^{0.5}$, as shown in Figure 5, where J is the current density, d is the thickness of the device, and V is the Voltage; $V = V_{\text{appl}} - V_{\text{bi}}$, where V_{appl} is the applied potential and V_{bi} is the built-in potential:

$$J_{\text{SCLC}} = \frac{9}{8}\varepsilon_o\varepsilon_r\mu_o\frac{(V - V_{bi})^2}{d^3}\exp[0.89\gamma\sqrt{\frac{V - V_{bi}}{d}}] \quad (1)$$

According to eq. (1)[26] and Figure 5, the hole mobilities of **P1** and **P2** were evaluated to be 5.96×10^{-4} and 9.67×10^{-4} $\text{cm}^2\ \text{V}^{-1}\ \text{s}^{-1}$, respectively. The results show that the polymers exhibited good hole mobility and would be suitable as polymer donor materials in PSCs. Because the hole mobility of PBDT–DODTBT was 7.15×10^{-3} $\text{cm}^2\ \text{V}^{-1}\ \text{s}^{-1}$,[14] **P1** displayed the lowest hole mobility among the three copolymers. **P2** exhibited a relatively lower mobility

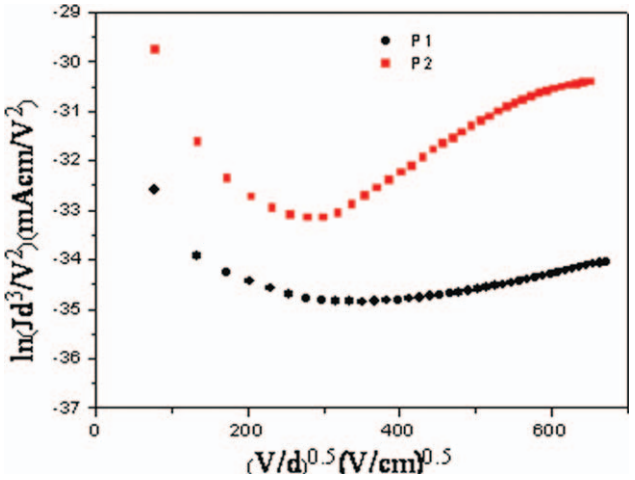

Figure 5 $\ln(Jd^3/V^2)$ versus $(V/d)^{0.5}$ plot of the copolymers for the measurement of hole mobilities by the SCLC method. [Color figure can be viewed in the online issue, which is available at wileyonlinelibrary.com.]

compared to that of PBDT–DODTBT; this may have been due to its random structure and low regioregularity. The results suggest that incorporation of thiophene units into the D–A conjugated polymer backbone may be a good way to improve hole mobility and could lead to enhanced device performance.

X-ray analysis

To evaluate the crystallinity of the polymers, XRD measurements were taken for the spin-coated films on SiO_2 substrate. Figure 6 shows the XRD spectra of the thin films of **P1** and **P2** at room temperature. It is clear that **P1** and **P2** exhibited a broad band centered around 15–40°; this indicated that the copolymers were amorphous.

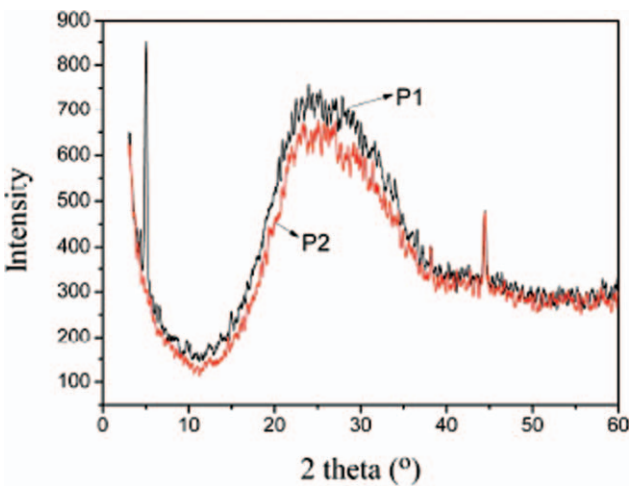

Figure 6 XRD patterns of the polymers in solid films. [Color figure can be viewed in the online issue, which is available at wileyonlinelibrary.com.]

TABLE II
Photovoltaic Properties of the PSC Devices

Polymer	Polymer–$PC_{71}BM$ (w/w)	V_{oc} (V)	J_{sc} (mA/cm²)	FF (%)	PCE (%)
P1	1 : 1	0.68	0.90	44.18	0.30
	1 : 2	0.66	1.84	41.82	0.51
P2	1 : 1	0.72	4.26	39.9	1.22
	1 : 2	0.74	3.94	53.30	1.55
	1 : 3	0.74	3.25	49.61	1.19
PBDT–DODTBT	1 : 1	0.80	5.40	54.40	2.35
	1 : 2	0.76	8.84	59.59	4.02

Photovoltaic properties

To investigate the photovoltaic properties of the polymers, photovoltaic devices with **P1, P2,** or PBDT–DODTBT as an electron donor and $PC_{71}BM$ as the electron acceptor were fabricated. The typical device structure was ITO/PEDOT:PSS/active layer/Ca (10 nm)/Al (100 nm). The devices were characterized under AM1.5G illumination (100 mW/cm²). The photovoltaic properties of the devices with different polymer/$PC_{71}BM$ weight ratios are summarized in Table II. The devices with a polymer/$PC_{71}BM$ weight ratio of 1 : 2 showed the best photovoltaic properties. Figure 7 shows the current density–voltage curves of the devices and the corresponding values of open-circuit voltage (V_{oc}), short-circuit current density (J_{sc}), and fill factor (FF); the PCEs were listed in Table II. At a 1 : 2 weight ratio of polymer to $PC_{71}BM$, the devices with **P1**/$PC_{71}BM$ as the active layer (75 nm) gave a V_{oc} value of 0.66

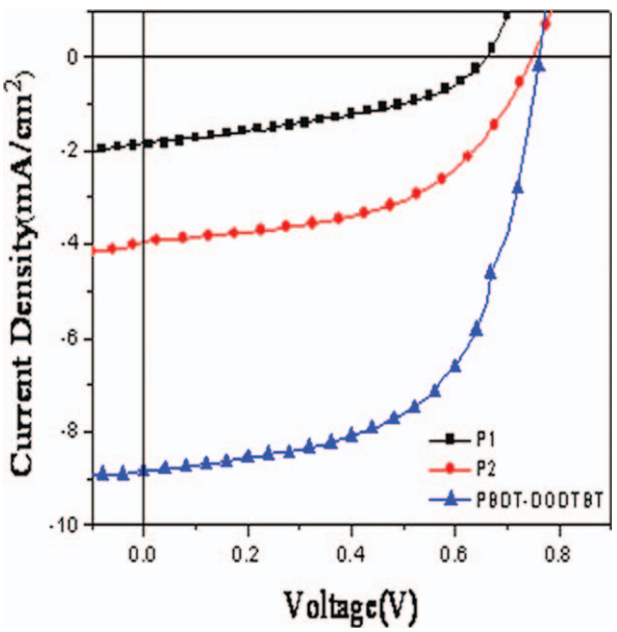

Figure 7 Current density–voltage curves of the devices. [Color figure can be viewed in the online issue, which is available at wileyonlinelibrary.com.]

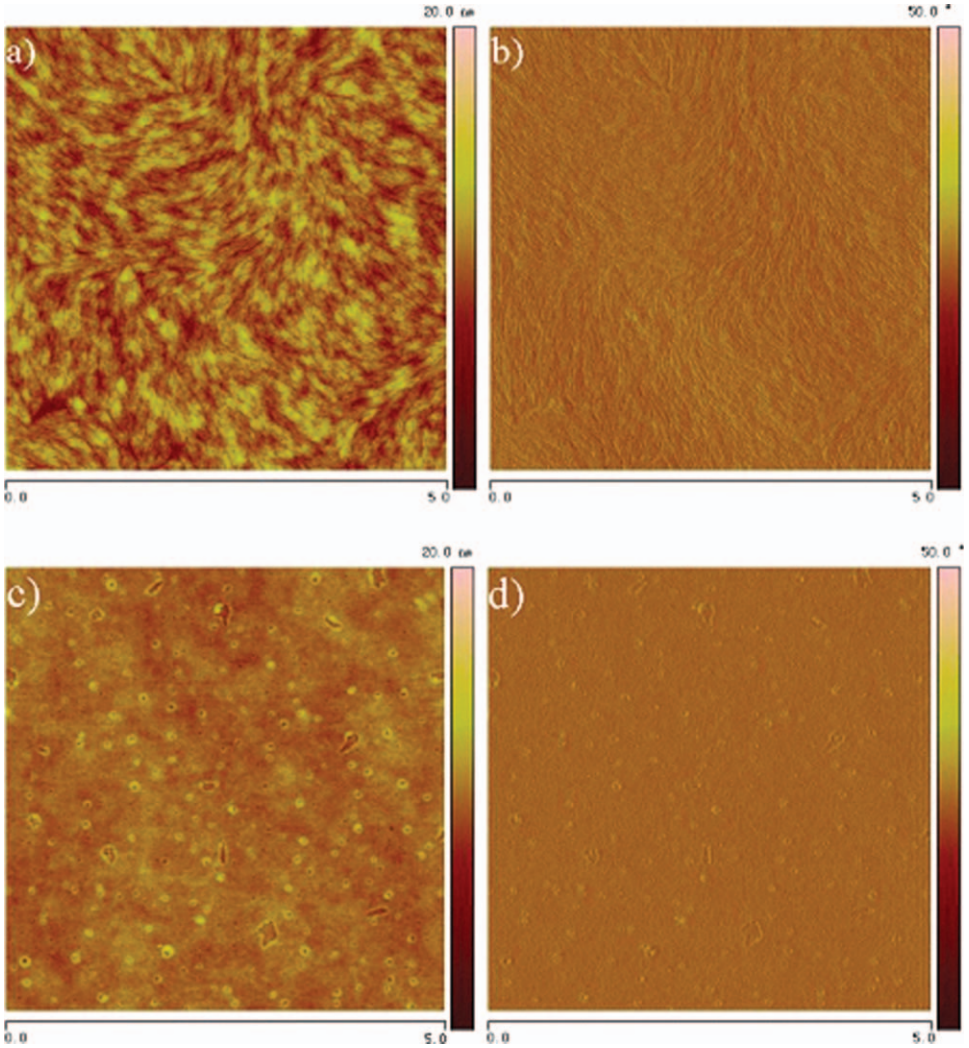

Figure 8 (a,c) AFM (5 × 5 μ m) topography and (b,c) phase images for the polymer–$PC_{71}BM$ blend films (1 : 2 w/w): (a,b) **P1**–$PC_{71}BM$ blend and (c,d) **P2**–$PC_{71}BM$ blend. [Color figure can be viewed in the online issue, which is available at wileyonlinelibrary.com.]

V, an FF of 41.82%, and a J_{sc} value of 1.84 mA/cm^2; this resulted in a PCE value of 0.51%. The devices with **P2**/$PC_{71}BM$ as the active layer (70 nm) showed a V_{oc} of 0.74 V, a J_{sc} of 3.94 mA/cm^2, and an FF of 53.30%; this resulted in a PCE of 1.55%. The devices with PBDT–DODTBT/$PC_{71}BM$ as an active layer (80 nm) exhibited a V_{oc} of 0.76 V, a J_{sc} of 8.84 mA/cm^2, an FF of 59.59%, and a PCE of 4%.

From the photovoltaic device results of **P1, P2,** and PBDT–DODTBT, we observed that V_{oc} was almost the same with the different polymer/$PC_{71}BM$, but J_{sc} exhibited a significant difference. The phenomenon confirmed that V_{oc} of the PSCs was directly related to the difference in LUMO of the electron acceptor and HOMO of the electron donor.[27] In comparison with **P1, P2** and PBDT–DODTBT exhibited relatively better photovoltaic performances. This may be explained by the fact that the incorporation of thiophene units into the conjugated polymer backbone favored light harvesting and enhanced hole mobilities and then gave a relatively higher J_{sc}. Furthermore, the lower LUMO energy levels of **P2** and PBDT–DODTBT were favorable for a decreasing energy level difference between the LUMO energy levels of the donor and PCBM; this could have decreased the energy loss upon exciton splitting.[28] **P2** showed a lower J_{sc} and FF compared to those of PBDT–DODTBT; this may have resulted from lower mobility and chain packing.

Morphology

Morphology is very important in the determination of the photovoltaic properties in PSCs. The morphologies of the blend films with a polymer/$PC_{71}BM$ blend ratio of 1 : 2 were investigated by AFM. As shown in Figure 8, all of the blend films showed a smooth surface with a root-mean-square roughness

of 1.06 nm for the **P1**/$PC_{71}BM$ blend and 0.61 nm for the **P2**/$PC_{71}BM$ blend; this indicated good miscibility between the copolymers and $PC_{71}BM$. In addition, the image mean roughness values of the **P1**/$PC_{71}BM$ film and **P2**/$PC_{71}BM$ film were 0.91 and 0.38 nm, respectively. From the phase images, the polymer and fullerene domains were homogeneously distributed throughout the blend film; in other words, a nanometer-scale interpenetrating network was formed in this blend; this could benefit not only the charge separation but also the charge transport and, therefore, could lead to a good FF of the PSCs.

CONCLUSIONS

In summary, two copolymers from substituted benzothiadiazole derivatives and BDT were synthesized by a Stille cross-coupling reaction; for comparison, the polymer PBDT–DODTBT was also introduced in this work. The incorporation of thiophene units showed some influence on the hole mobilities, morphologies, and photovoltaic properties of DOBT-based copolymers. Preliminary investigations of the PSCs with ITO/PEDOT:PSS/polymer:$PC_{71}BM$/Ca/Al were done. The polymer/$PC_{71}BM$ weight ratio of 1 : 2 showed the best photovoltaic properties, and the PCE of the device based on **P2**/$PC_{71}BM$ with a weight ratio of 1 : 2 reached 1.55%. This indicated that **P2** was a promising candidate for PSCs. The optimization of structures with high regioregularity, the molecular weights of DOBT-based polymers, and the morphologies of the blends are believed to further enhance the photovoltaic performance of this kind of polymers.

The authors acknowledge Bo Liu and Bo Peng for the synthesis of the intermediates and some characterizations of the polymers and also helpful discussions from Yongfang Li.

References

1. Yu, G.; Gao, J.; Hummelen, J. C.; Wudl, F.; Heeger, A. J. Science 1995, 270, 1789.
2. Chen, H.; Huang, H.; Tian, Z.; Shen, P.; Zhao, B.; Tan, S. Eur Polym J 2010, 46, 673.
3. Li, Y.; Zou, Y. Adv Mater 2008, 20, 2952.
4. Liu, B.; Zou, Y.; Peng, B.; Zhao, B.; Huang, K.; He, Y.; Pan, C. Polym Chem 2011, 2, 1056.
5. Zhou, H.; Yang, L.; Price, S.; Knight, K.; You, W. Angew Chem Int Ed 2010, 49, 7992.
6. Woo, C.; Beaujuge, P.; Holcombe, T.; Lee, O.; Frechet, J. M. J Am Chem Soc 2010, 132, 15,547.
7. Cheng, Y.; Yang, S.; Hsu, C. Chem Rev 2009, 11, 5868.
8. Hou, J. H.; Park, M. H.; Zhang, S. Q.; Yao, Y.; Chen, L. M.; Li, J. H.; Yang, Y. Macromolecules 2008, 41, 16.
9. Liang, Y. Y.; Xu, Z.; Xia, J. B.; Tsai, S. T.; Wu, Y.; Li, G.; Ray, C.; Yu, L. P. Adv Mater 2010, 22, E135.
10. Chen, H.; Hou, J.; Zhang, S.; Liang, Y.; Yang, G.; Yang, Y.; Yu, L.; Wu, Y.; Li, G. Nat Photonics 2009, 3, 649.
11. Zou, Y.; Najari, A.; Berrouard, P.; Beaupré, S.; Aich, R. B.; Tao, Y.; Leclerc, M. J Am Chem Soc 2010, 132, 5330.
12. Najari, A.; Beaupré, S.; Berrouard, P.; Zou, Y.; Pouliot, J.; Pérusse, C.; Leclerc, M. Adv Funct Mater 2011, 21, 718.
13. Piliego, C.; Holcombe, T. W.; Douglas, J. D.; Woo, C. H.; Beaujuge, P. M.; Frechet, J. M. J. J Am Chem Soc 2010, 132, 7595.
14. Ding, P.; Chu, C. C.; Liu, B.; Peng, B.; Zou, Y. P.; He, Y. H.; Zhou, K. C.; Hsu, C. S. Macromol Chem Phys 2010, 211, 2555.
15. Pei, J.; Yu, W. L.; Huang, W. Macromolecules 2000, 33, 2462.
16. Li, Y. W.; Xue, L. L.; Xia, H. J.; Xu, B.; Wen, S. P.; Tian, W. J. J Polym Sci Part A: Polym Chem 2008, 46, 3970.
17. Zhao, G. J.; He, Y. J.; Li, Y. F. Adv Mater 2010, 22, 4355.
18. Liang, Y.; Wu, Y.; Feng, D.; Tsai, S. T.; Son, H. J.; Li, G.; Ray, C.; Yu, L. J Am Chem Soc 2009, 131, 56.
19. Yang, M.; Peng, B.; Liu, B.; Zou, Y. P.; Zhou, K. C.; He, Y. H.; Pan, C. Y.; Li, Y. F. J Phys Chem C 2010, 114, 17, 989.
20. Blouin, N.; Leclerc, M. Acc Chem Res 2008, 41, 1110.
21. Sun, Q.; Wang, H.; Yang, C.; Li, Y. J Mater Chem 2003, 13, 800.
22. Zou, Y.; Sang, G.; Wu, W.; Liu, Y.; Li, Y. Synth Met 2009, 159, 182.
23. Liu, B.; Najari, A.; Pan, C. Y.; Leclerc, M.; Xiao, D.; Zou, Y. Macromol Rapid Commun 2010, 31, 391.
24. Cho, S.; Seo, J. H.; Kim, S. H.; Song, S.; Jin, Y.; Lee, K.; Suh, H.; Heeger, A. J. Appl Phys Lett 2008, 93, 263301.
25. Blouin, N.; Michaud, A.; Gendron, D.; Wakim, S.; Blair, E.; Plesu, R. N.; Belletete, M.; Durocher, G.; Tao, Y.; Leclerc, M. J Am Chem Soc 2008, 130, 732.
26. Martens, H. C. F.; Brom, H. B.; Blom, P. W. M. Phys Rev B., 1999, 60, 8489.
27. Mihailetchi, V. D.; Blorn, P. W. M.; Hummelen, J. C.; Rispens, M. T. J Appl Phys 2003, 94, 6849.
28. Koster, L. J. A.; Mihailetchi, V. D.; Blom, P. W. M. Appl Phys Lett 2006, 88, 3511.